



**Pre-normative REsearch for Safe use of Liquid Hydrogen (PRESLHY)**

Project Deliverable

## **Summary of experiment series E5.3 (Cold Channel)**

Deliverable Number:	D5.6
Work Package:	5
Version:	1.1
Author(s), Institution(s):	A. Friedrich, PS; A. Vesper, PS; J. Gerstner, PS; J. Rietz, KIT and T. Jordan, KIT
Submission Date:	30 July 2021
Due Date:	
Report Classification:	Confidential



**FUEL CELLS AND HYDROGEN**  
JOINT UNDERTAKING



This project has received funding from the Fuel Cells and Hydrogen 2 Joint Undertaking under the European Union's Horizon 2020 research and innovation programme under grant agreement No 779613.

History		
Nr.	Date	Changes/Author
1.0	30.05.2021	Original version by A. Friedrich, A. Vesper, J. Gerstner and T. Jordan PS/KIT
1.1	11.08.2021	Updated test matrix (cannula-corrected cH <sub>2</sub> -values taken from data sets, not uncorrected values from protocol) and updated pages in table of contents. 2 sentences on cH <sub>2</sub> -correction and equation (2) in the text. A. Friedrich

Approvals			
Version	Name	Organisation	Date
1.1	T. Jordan	KIT	11.08.2021

## Acknowledgements, Preface and Disclaimer

This project has received funding from the Fuel Cells and Hydrogen 2 Joint Undertaking under the European Union’s Horizon 2020 research and innovation programme under grant agreement No 779613.

This report deals with more than 100 combustion experiments with cryogenic hydrogen-air-mixtures in a semi-confined obstructed channel.

This report contains the “meta data” of the respective experiments, providing detailed description of the experimental set-up, sensors and result data storage. The actual result data will be provided via KITopen. Detailed evaluation of the results, as well as any modelling work is excluded here and left for subsequent work.

Because of the interrelation with the published result data it is intended to turn this confidential report into a public one.

Despite the care that was taken while preparing this document the following disclaimer applies: The information in this document is provided as is and no guarantee or warranty is given that the information is fit for any particular purpose. The user thereof employs the information at his/her sole risk and liability.

The document reflects only the authors’ views. The FCH JU and the European Union are not liable for any use that may be made of the information contained therein.

## Key words

Cryogenic hydrogen-air-mixtures, ignition, concentration gradient, semi-confined geometry

## **Publishable Short Summary**

In the frame of the PRESLHY project more than 100 combustion experiments with cryogenic hydrogen-air-mixtures were made in a semi-confined obstructed channel. In the experiments a large H<sub>2</sub>-concentration range from 10 vol% up to 60 vol% as well as different blockage ratios (BR = 0, 30 and 60%) were investigated. Besides the main experiment series at cryogenic temperatures (approx. 100 K inside the channel) most of the experiments were also performed at ambient temperature for comparison.

## Table of Contents

Acknowledgements, Preface and Disclaimer.....	ii
Key words.....	iii
Publishable Short Summary .....	iv
Table of Contents.....	v
<b>1 Purpose of the Tests – Knowledge Gap Addressed.....</b>	<b>1</b>
<b>2 Experimental setup.....</b>	<b>2</b>
2.1 Cooling tube.....	3
2.2 Combustion channel .....	4
2.2.1 Obstacles .....	4
2.2.2 Ignition wall and ignition device .....	5
<b>3 Experimental procedure and Instrumentation .....</b>	<b>6</b>
3.1 Experimental procedure .....	6
3.2 Instrumentation in distribution experiments .....	7
3.2.1 H <sub>2</sub> -concentration measurements.....	7
3.2.2 Temperature measurements .....	9
3.3 Instrumentation in combustion experiments .....	9
3.4 Optical instrumentation .....	11
3.5 Estimate of Measurement Errors.....	12
<b>4 Test matrix and data structure of Cold-Channel-Experiments .....</b>	<b>13</b>
4.1 Structure of the Datasets .....	19
<b>5 Summary, Conclusions and Outlook.....</b>	<b>22</b>

## 1 Purpose of the Tests – Knowledge Gap Addressed

Main goal of the Cold Channel Experiments is to evaluate the hazard of accelerated flame propagation over a spill of LH2 in presence of a vertical hydrogen concentration gradient at cryogenic temperatures.

The tests were performed in a half open box 3 x 0.6 m<sup>2</sup> with a height of 0.4 m, whose ceiling was located approximately 2 m above the ground level of a concrete pit on the free field test site north of KIT Campus North, which was the main test field for the KIT / PS experimental sub-program of the PRESLHY project. The test site is located in a forest environment approx. 2 km north of the KIT Campus North. The next inhabited buildings provide a similar distance of approximately 2 km (see Figure 1).



*Figure 1: Location (left) and aerial view from the north (right) of the free-field test site north of KIT Campus North with position of the concrete pit (red rectangle).*



*Figure 2: View into the concrete pit from a position above the channel in the direction of the location of the data-acquisition (behind blue container).*

On the test site a large concrete pit is available from an earlier project. The pit with a length of approx. 100 m, a width of 5 m and a depth of 4 m is embedded in the ground and it is protected against the weather by a large foldable tent. The combustion channel utilized in the current test series is assembled at one end of the pit using the narrow pit side to fasten the background needed for the optical observations with the BOS-technique. Figure 2 shows a photograph of the interior of the concrete pit.

In the tests it was aimed to ignite H<sub>2</sub>-air mixtures with concentration gradients similar to the natural hydrogen concentration gradients above a spill of LH<sub>2</sub>. Together with the H<sub>2</sub>-concentration gradients temperature profiles were created in the combustion channel. The gas mixtures were ignited in positions with high hydrogen reactivity and flame propagation velocities were measured in configurations with and without obstacles in the flame path.

To generate the test mixtures cold hydrogen with a temperature of approx. 80 K (boiling temperature of liquid nitrogen (LN<sub>2</sub>)) was injected from the LN<sub>2</sub>-cooled channel ceiling into the channel volume. To determine the concentration and temperature profiles generated inside the channel, measurements of local hydrogen concentration and temperature profiles were performed in distribution experiments. In the subsequent combustion experiments, in which the mixture was ignited, pressure sensors and high-speed video combined with BOS technique were used to capture the characteristics of the combustion behavior.

## 2 Experimental setup

The Cold-Channel-facility mainly consists of a steel-tube for gas pre-cooling in a bath of LN<sub>2</sub> and the combustion channel with an LN<sub>2</sub>-cooled ceiling. To the cooled ceiling injection lines are fastened from below, which are fed with cold H<sub>2</sub> from the cooling tube via LN<sub>2</sub>-cooled filling lines. Figure 3 and Figure 4 show a sketch and photos of the setup of the Cold-Channel-facility.

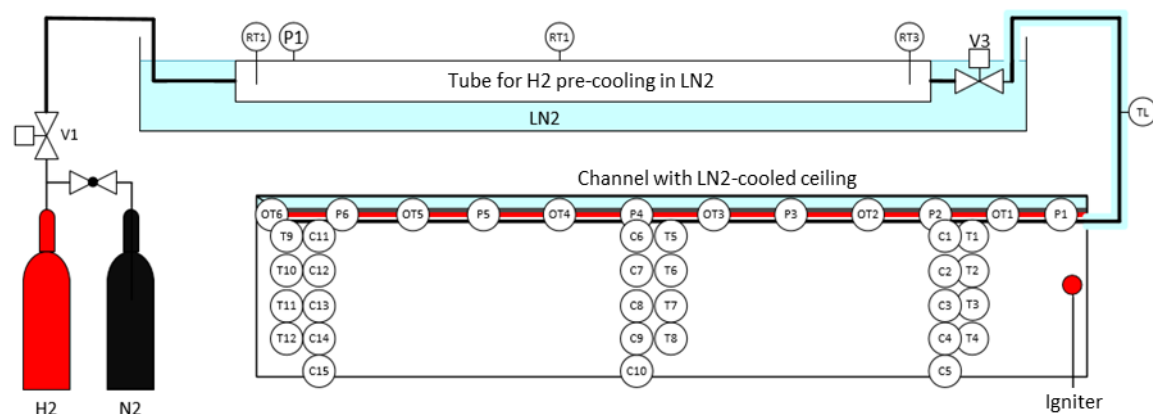


Figure 3: Sketch with main parts of the Cold-Channel-facility.



*Figure 4: Photo of the Cold-Channel facility (top) and detail of the combustion channel (bottom).*

## 2.1 Cooling tube

The cooling tube is a 5 m long stainless-steel tube with an inner diameter of 54 mm and a wall thickness of 9.5 mm (see Figure 5). It was designed for a test series on the combustion regimes of cryogenic H<sub>2</sub>-air mixtures (see PRESLHY D3.4 on E5.2 results) and is designed for pressures up to 70 bar at the boiling temperature of LN<sub>2</sub> (80 K). In its current application the tube is equipped with one pressure sensor (WIKA, Type S-20, 0 - 250 bar) and two thermocouples (KIT-Workshop, Type K, d = 1 mm) to monitor the initial conditions of the pre-cooled H<sub>2</sub> that is later injected into the combustion channel.



*Figure 5: Photo of the cooling tube after fabrication*

## 2.2 Combustion channel

The combustion channel has a length of 3 m, a height of 40 cm and a width of 60 cm and is hanging from a welded support structure that holds its ceiling at a height of approx. 2 m above the ground level (Figure 4). The channel has an open ground face and can be equipped with eleven obstacles (two sets of obstacles for blockage ratios of 30% and 60% were fabricated) with a spacing of 250 mm. For optical observation the sidewalls of the combustion channel are made of transparent Makrolon plates (thickness 11 mm) that are stabilized by eleven frame structures around the channel cross section in the obstacle positions. The ceiling of the channel is made of an aluminium plate fastened to four aluminium channels (cross section 120 mm x 40 mm) that allow cooling of the top plate with LN2 (Figure 6 and Figure 11). On its ignition end, the channel is closed tightly by a metal sheet, while its opposite end is open, but sealed by a thin plastic film in the experiments.

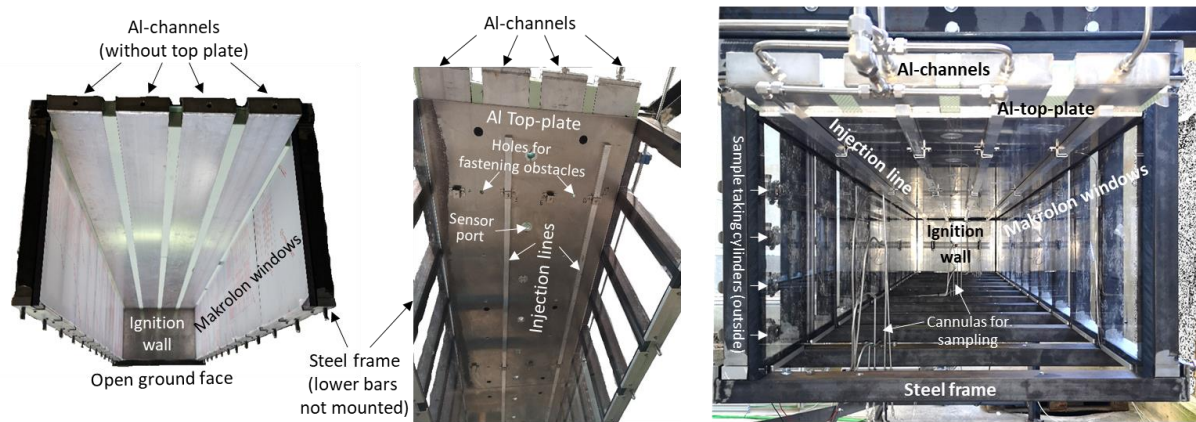


Figure 6: Inside views of the combustion channel from the open end and from below during construction (left and center) and during distribution experiments with the unobstructed channel (right).

Along the pre-cooled channel ceiling four aluminium injection lines with rectangular cross-section (inner dimensions 11 mm x 16 mm) are positioned. The material was chosen to also cool the lines through the contact with the pre-cooled channel ceiling. The cold hydrogen provided by the cooling tube is released through 96 holes (12 holes on either side of every injection line) with a diameter of 2 mm in horizontal direction into the combustion channel. The holes are located in distances of 25 cm to each other with the first hole having a distance of 25 cm to the ignition wall. With the horizontal release it is intended to generate a stratified H<sub>2</sub>-air-mixture with a vertical H<sub>2</sub>-concentration gradient inside the channel, that is ignited in the main experimental series. To control the formation of the stratified mixture distribution experiments were performed, in which gas samples were taken at the point in time when the ignition is planned in the combustion experiments.

### 2.2.1 Obstacles

The obstacles in the channel are accelerating the flame by generating turbulence. Two sets of eleven obstacles with blockage ratios of 30% and 60% of the channel cross-sectional area were fabricated. The obstacles are designed to withstand the combustion loads, but nevertheless, in case of failure, they should cause as little damage as possible to the Makrolon windows.

So tiny wooden bars with a cross section of 15 mm x 25 mm and a length of 557 mm were used, which block an area of  $15 \times 557 = 8355 \text{ mm}^2$  per bar in the orientation they were mounted to the channel. The channel itself has a cross sectional area of  $240.000 \text{ mm}^2$  and thus, theoretically, approximately 8.6 wooden bars are required for a blockage rate (BR) of 30% and approximately 17.2 wooden bars for a BR of 60%. Since the bars have to be positioned above each other via spacers it was decided to use six wooden bars for the obstacles with a BR of 30%, and 13 wooden bars for the obstacles with BR 60%. The remaining cross-sectional area to be obstructed is blocked by spacers of the thickness 25 mm (BR 30%: 80 spacers measuring  $18.23 \times 15 \text{ mm}^2$ ; BR 60%: 24 outer spacers  $25 \times 15 \text{ mm}^2$  and 24 inner spacers  $73.29 \times 15 \text{ mm}^2$ ), as sketched in Figure 7.

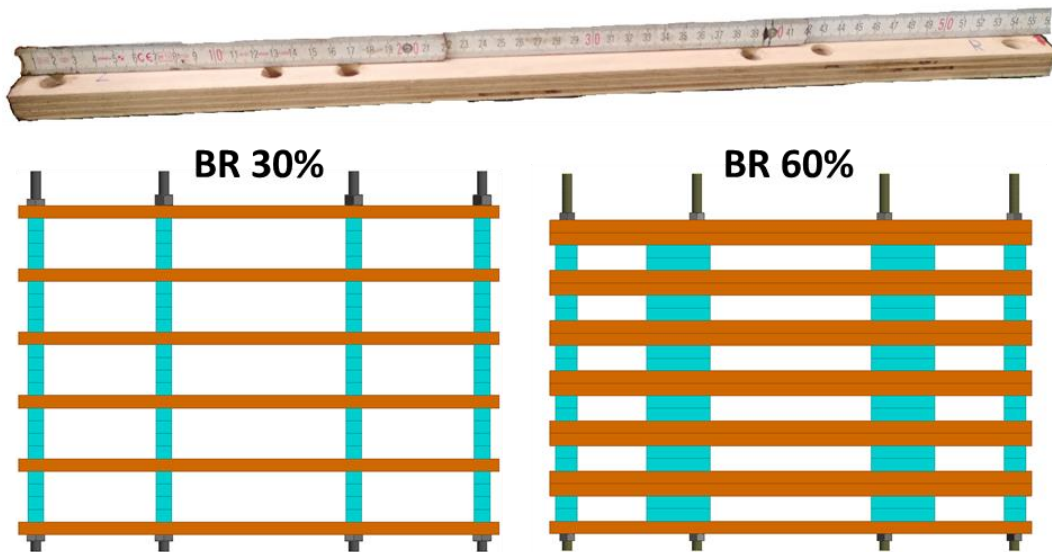


Figure 7: Wooden bar for fabrication of obstacles (top) and obstacle geometry with bars (brown) and spacers (blue) for blockage ratios of 30% (bottom left) and 60% (bottom right).

Bars and spacers are connected by four threaded rods to form individual parts that can be inserted easily into the combustion channel. On their top the threaded rods are fastened to the top plate of the channel with nuts, while their lower end is connected with the lower bar of the steel frame around the channel in the obstacle positions (see Figure 6 bottom right).

### 2.2.2 Ignition wall and ignition device

The ignition wall (see Figure 6 and Figure 8) must tightly cover the entire cross-sectional area of the ignition end of the channel. Therefore, it is made from a stainless-steel plate with a thickness of 8 mm and the dimensions  $60 \times 40 \text{ cm}^2$  (see Figure 8 top left). It is fastened to a supporting frame and has seven sets of holes for positioning the ignition device in different heights to allow an ignition in regions with different hydrogen concentrations in the experiments with vertical  $\text{H}_2$ -concentration gradients. The spare holes in the ignition wall that were not used by the ignition device were closed with screws during the experiments. In all experiments of the series described here the ignition device is positioned in the same height of 50 mm below the channel ceiling.

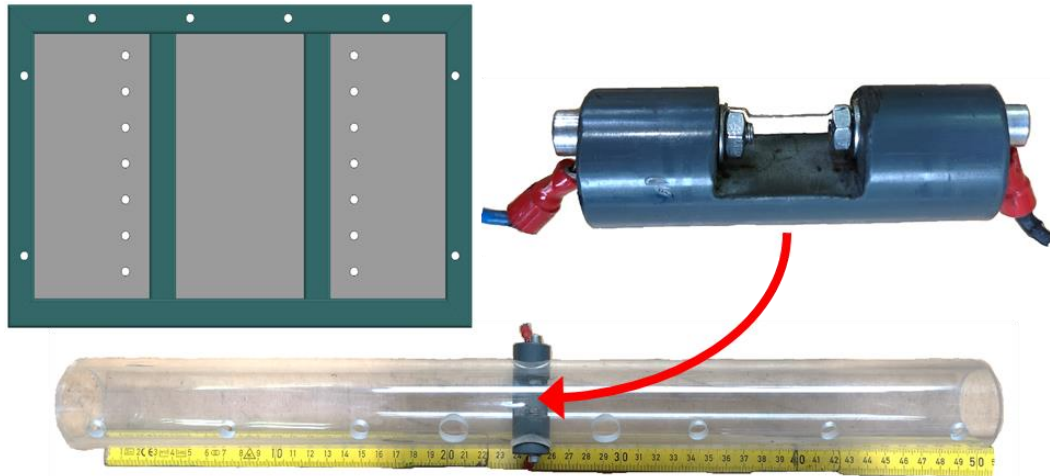


Figure 8: Ignition end wall (top left) and ignition device.

As ignition device a glow wire in a perforated tube ( $d_i = 50 \text{ mm}$ ,  $l = 500 \text{ mm}$ ) is used. The glow wire ignites the mixture inside the tube and the flame then propagates primarily through the tube, but also leaves it through the holes in its circumference. In this way the flame is spread over the entire channel width within a relatively short distance to the ignition wall. Since the glow wire is destroyed during the ignition it has to be replaced for each experiment.

### 3 Experimental procedure and Instrumentation

In principle two experimental series with emphasis on different phenomena were performed with the Cold-Channel facility:

- distribution experiments on  $\text{H}_2$ -concentration gradient and temperature profile formation in the channel, and
- ignited experiments on the combustion behaviour of the gradient mixtures characterized in the distribution experiments.

In most cases the ignited experiments were carried out immediately after a successful distribution test with exactly the same initial settings. To allow such fast changes in the scope of the experiments the facility was constructed in a way that allowed fast modifications to the instrumentation used in the tests.

#### 3.1 Experimental procedure

Prior to each experiment (either distribution or combustion and either at ambient or cryogenic temperature) the open end wall of the facility is sealed with a thin plastic film, and, in case of a combustion experiment, a glow wire is installed to the ignition system. For experiments at cryogenic temperature the box around the cooling tube and all lines that are equipped with an encasement for cooling as well as the cooling profiles above the ceiling of the combustion channel are filled with  $\text{LN}_2$ . When the desired temperature levels have established, the cooling tube is filled with  $\text{H}_2$  at defined temperature and pressure conditions. To control these initial conditions the signals of the pressure sensor (WIKA, Type S-20, 0 - 250 bar) and the two thermocouples (KIT-Workshop, Type K,  $d = 1 \text{ mm}$ )

installed to the tube are displayed at the control computer and also recorded with the slow LabView data acquisition system. From the control computer also all valves of the facility are operated to allow a thorough approach to the intended values for the initial tube conditions, with several breaks to establish thermal equilibrium inside.

After the initial conditions in the cooling tube have reached the targeted values the experimental parameters are entered into the experiment control programme. These parameters are the H<sub>2</sub>-injection duration (for control of injected H<sub>2</sub>-amount) and the ignition delay time and its duration in the combustion experiments, which coincides with the time of the sample withdrawal for the H<sub>2</sub> concentration measurements in the distribution experiments. Then the automated experimental procedure is started on the control computer, with the fast data acquisition and the high-speed camera being activated beforehand in waiting-for-trigger-mode (only in combustion experiments). The procedure then controls the injection process and, after the specified delay time, activates the sample taking process (distribution experiment) or the ignition (combustion experiment) together with a trigger signal to the fast data acquisition system and the high-speed camera. During an experiment all personnel either leaves the concrete pit or hides in the control area behind a concrete filled container inside the pit in a distance of approx. 30 m (compare Figure 2).

### 3.2 Instrumentation in distribution experiments

#### 3.2.1 H<sub>2</sub>-concentration measurements

For the determination of the H<sub>2</sub>-concentration profiles generated in the combustion channel distribution experiments were performed, in which several gas samples were taken from the channel atmosphere at the point in time in which the mixture is ignited in the corresponding combustion experiments. The samples were taken using 12 sample taking cylinders (V = 16 ml) that were positioned in three rows of 5 cylinders outside the channel and extracted the sample from the sampling point inside the channel through a thin cannula (d<sub>i</sub> = 1 mm, l = 800 mm). The gas extraction positions of the cylinders with their names in the data files are sketched in Figure 9.

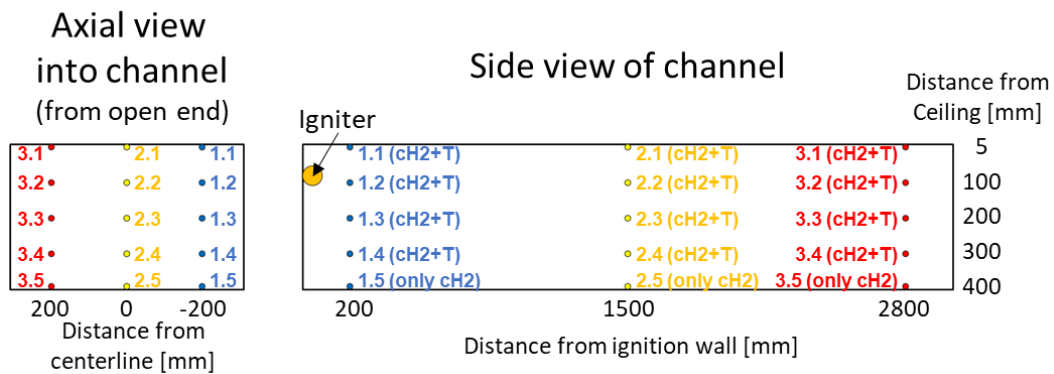


Figure 9: Sketch of numbering of gas sampling and temperature measurement positions in distribution experiments: View from the open channel end into the channel (left) and side view (right).

All sample taking cylinders were equipped with two valves. The remote-controlled inlet valve is connected via the cannula to the sampling position inside the channel, while the

hand valve is equipped with a quick connector for either evacuating the cylinder using a portable vacuum pump, or to connect it to the H<sub>2</sub>-sensor (with pump) for sample evaluation. The evacuation of the cylinders as well as the evaluation of the samples is performed manually (cylinder by cylinder) prior to and directly after an experiment, while the sample taking process at the pre-set point in time is initiated remotely using the experiment control computer. A photo of one row with 4 cylinders at its position outside the channel and a photo with all components used for the H<sub>2</sub>-concentration measurements (in an assembly as used for the calibration tests, see below) are shown in Figure 10.

When a sample is taken, the gas volume that is already present in the cannula is also sucked into the sample taking cylinder. This gas had already been in the cannula prior to the start of the experiment and thus does not contain any hydrogen. To keep the error caused by this volume constant in all measurement positions, all cannulas are of the same length and diameter ( $l = 800 \text{ mm}$  and  $d_i = 1 \text{ mm}$ ) and thus have a volume of

$$V_{ca} = \pi \cdot d_i^2/4 \cdot l = 0.628 \text{ ml} \quad (1)$$

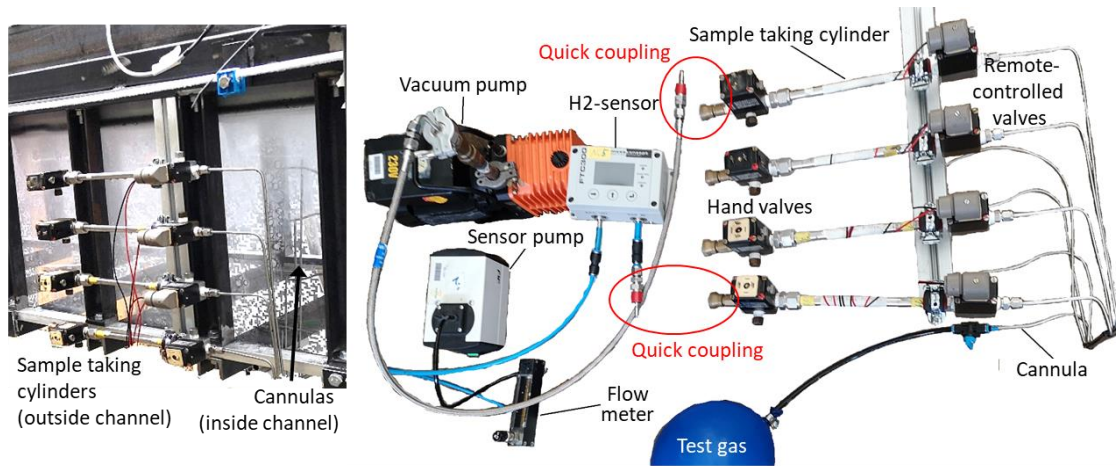


Figure 10: Photo of one cylinder row at its position outside the channel (left) and photo of all components used for the H<sub>2</sub>-concentration measurements in an assembly as used for the calibration tests (right).

To quantify the influence of the cannula volume on the hydrogen concentration measurements calibration tests were performed with a test gas of known composition (forming gas, 90 Vol% N<sub>2</sub> and 10 Vol% H<sub>2</sub>). In the tests a balloon with the test gas is connected to the evacuated sample taking cylinder via a cannula that is filled with ambient air, thus providing identical initial conditions as for a concentration measurement in a real distribution test. When the measurement is triggered, the test gas is sucked into the cylinder together with the gas of the cannula volume, causing the same measurement error as in a real experiment. Every set of sample taking cylinder and cannula used in the facility was tested twice in this way during the calibration tests – results are provided in Appendix 1 - and only a negligible difference was found in between the measurements with different sampling cylinders. But a systematic error of approx. 4% of the measured value (analysis only detects 96% of real H<sub>2</sub> concentration value) can be clearly attributed to the cannula volume, which corresponds very good with the volume fraction of the cannula compared to the cylinder volume ( $V_{cy} = 16 \text{ ml} \rightarrow V_{ca} = 0.628 \text{ ml} \approx 0,039 \cdot V_{cy}$ ). So prior to publication all concentration values were corrected using the following equation:

$$c_{H_2_{published}} = c_{H_2_{measured}} \cdot 100/96 \quad (2)$$

All samples taken during an experiment were evaluated with the portable H<sub>2</sub>-sensor directly after an experiment. The concentration courses of the measurements were recorded, but the maximum values measured for every sample were noted down during evaluation in an Excel-file that was generated also as a kind of protocol of the test campaign. In case the initial channel conditions desired were met by the concentration measurements, an ignited experiment was carried out immediately after the distribution experiment. In the ignited experiments the complete setup for cH<sub>2</sub>-measurements (cylinders and cannulas) was removed from the facility since the equipment might be damaged during the combustion process and it also disturbs the records of the various cameras that are used to monitor the tests.

### 3.2.2 Temperature measurements

In the distribution experiments also the temperature gradients generated inside the channel by the injection of the pre-cooled hydrogen are measured. To this end, 12 thermocouples (Type K, 1 mm), are positioned close to the cannula positions (see Figure 9) in the combustion channel in the three rows.

### 3.3 Instrumentation in combustion experiments

All sensors described in this chapter remained in the facility in every experiment (also in distribution tests), but were only recorded in case of a combustion experiment.

For the determination of the flame velocity and the pressure loads generated during the combustion the combustion channel is equipped with 6 open thermocouples (OT1 – OT6 in Figure 11) for flame detection and 6 pressure sensors (P1 – P6) that are located on the centerline of the channel ceiling in a central position in between two obstacles. Further 3 pressure sensors (P7 – P9) are positioned in lead bricks at the bottom of the concrete pit in a distance of approximately 2 m to the channel ceiling. At a later stage additionally 6 ionization probes (IP1 – IP6) were installed to the uppermost bar of every second obstacle along the channel centerline. The details and coordinates of all sensors with respect to the coordinate system sketched in the left part of Figure 11 are given in Table 1.

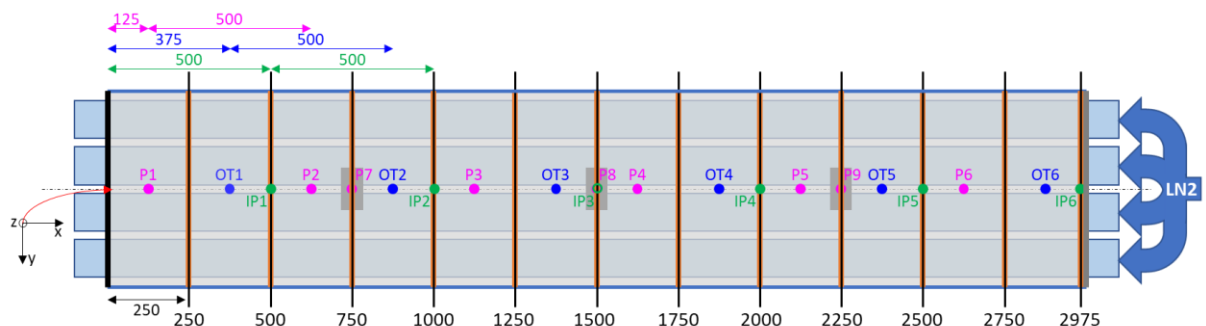


Figure 11: Sketch of the channel with the sensors used (obstacles are represented by brown lines).

Table 1: Positions and details of the sensors used in the Combustion channel

Sensor	Manufacturer	Type	Range	x [mm]	y [mm]	z [mm]
OT1	KIT-WS	Only flame detection		375	0	0
OT2	KIT-WS	Only flame detection		875	0	0
OT3	KIT-WS	Only flame detection		1375	0	0
OT4	KIT-WS	Only flame detection		1875	0	0
OT5	KIT-WS	Only flame detection		2375	0	0
OT6	KIT-WS	Only flame detection		3875	0	0
P1	PCB	112A05	0 – 35 bar	125	0	0
P2	PCB	112A05	0 – 35 bar	625	0	0
P3	PCB	112A05	0 – 35 bar	1125	0	0
P4	PCB	112A05	0 – 35 bar	1625	0	0
P5	PCB	112A05	0 – 35 bar	2125	0	0
P6	PCB	112A05	0 – 35 bar	2625	0	0
P7	PCB	112A05	0 – 35 bar	750	0	-2000
P8	PCB	112A05	0 – 35 bar	1500	0	-2000
P9	PCB	112A05	0 – 35 bar	2250	0	-2000
IP1	In-house	Only flame detection		500	0	0
IP2	In-house	Only flame detection		1000	0	0
IP3	In-house	Only flame detection		1500	0	0
IP4	In-house	Only flame detection		2000	0	0
IP5	In-house	Only flame detection		2500	0	0
IP6	In-house	Only flame detection		2975	0	0

In the combustion experiments additional open thermocouples (Type K, 2 mm, OT1 – OT6 in Figure 11) were positioned in the channel ceiling via adapters that were mounted in plane with the ceiling. Only the open part of the thermocouple is exposed to the propagating flame. The open thermocouples were fabricated at the KIT workshop using commercially available raw material (RECKMANN Mess- und Regeltechnik). To fabricate open thermocouples the protective metal shell around the tip of a closed thermocouple is removed and the temperature sensitive weld spot, that interconnects the two wires of different materials, is exposed directly to the surrounding medium (Figure 12). Without the protective shell the open thermocouples react much faster on temperature changes, but become much more vulnerable to pressure effects, corrosion and mechanical stress.

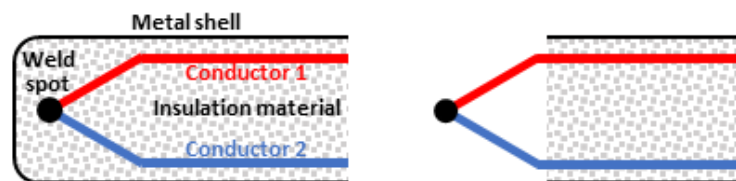


Figure 12: Sketch of a closed (left) and an open (right) thermocouple.

In the current application the open thermocouples were not used for precise temperature measurements and thus they were operated in a different circuit that produces a fast and more intense signal, which is no longer proportional to the temperature, but merely indicates a sharp change in temperature. A photo of a thermocouple in its fixation is shown in the left part of Figure 13.

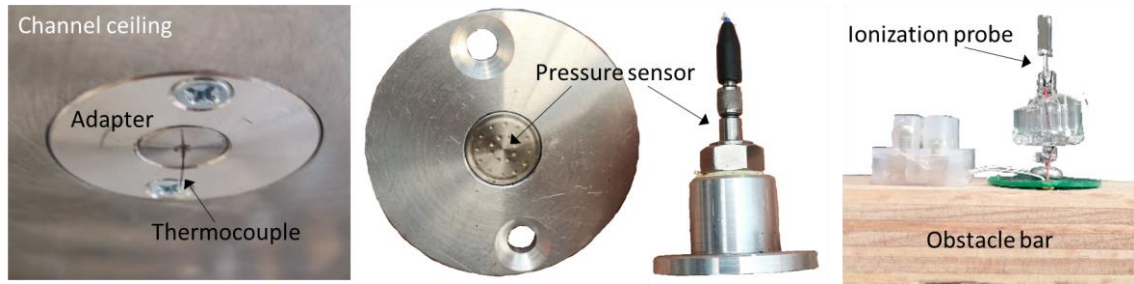


Figure 13: Photos of the different sensor fixations in the combustion channel.

The pressure sensors inside the channel (PCB, type 112A05, range 0 – 35 bar, P1 – P6 in Figure 11) were mounted in similar adapters as the open thermocouples, with their sensitive membrane in the same plane as the channel ceiling (Figure 13, center). The pressure sensors are also sensitive to temperature changes and thus the high temperature of the flame causes a strong negative signal drift in the moment the flame reaches the position of a pressure sensor. To protect the sensors the membranes were covered with a thin film of silicon grease during the experiments, but nevertheless the pressure records can also be used to determine the arrival time of a flame at the respective position due to the temperature effect. All pressure sensors were used with special signal converters that were delivered together with the sensors. The calibration data of the sensors and signal converters provided by the manufacturer are summarized in Appendix 2.

The ionization probes were directly fastened to the upper surface of the uppermost bar in every second obstacle of the channel (Figure 13, right). Ionisation probes consist basically of a capacitor and two metal contacts. The capacitor is charged and as long as there is only air (or hydrogen-air mixture) in between the contacts no current flow is possible. But as soon as a flame with ions and radicals in the reaction zone reaches the ionisation probe, charge transfer becomes possible and the capacitor is discharged. This discharge can be recognized as sudden voltage increase in the sensor records.

### 3.4 Optical instrumentation

Using the Background-Oriented-Schlieren (BOS) method, the invisible hydrogen flame can be visualized on its path through the channel. For this method, apart from a (high-speed) camera, only a background pattern behind the object of interest is needed. As can be seen in Figure 14 a background with a random pattern of black and white dots is mounted to the concrete wall in a distance of approx. 1.5 m besides the channel. Prior to an experiment a set of so-called reference images without hydrogen is taken with the camera from the opposite side of the channel. In these and all following images the background pattern (not the channel structure) is focussed, since density gradients, caused by the light gas hydrogen or a flame in the channel, lead to a shift of dot-arrays with respect to the reference image. The shifts can be quantified and plotted using algorithms similar to the ones used in PIV (Particle-Image-Velocimetry) to yield processed photos in which the gas cloud or flame is visible.



Figure 14: Side view of the channel with BOS-pattern in background.

### 3.5 Estimate of Measurement Errors

Table 2 provides the accuracies of the sensors used in the experiments. The values were taken from the respective manuals for ambient temperature conditions. For cryogenic temperatures no data is available.

Table 2: Accuracy of the sensors used in the Cold channel experiments

Sensor	Manufacturer	Type (Range)	Non-linearity @ 290 K
Pressure (PV & PN)	WIKA	S-20 (250 bar)	< 0,125% FS
Pressure (P1 & P5)	PCB	112A22 (3.5 bar)	$\leq 1\%$ FS
Pressure (P2 – P4)	PCB	113B21 (14 bar)	$\leq 1\%$ FS
Pressure (P6)	PCB	113B28 (3.5 bar)	$\leq 1\%$ FS
Temperature	KIT-Workshop	Type K, d = 0.36 mm	1.66 °C

All closed thermocouples used for temperature measurements were calibrated in ice-water ( $T = 273$  K), solid CO<sub>2</sub> ( $T = 194,67$  K) and LN<sub>2</sub> ( $T = 70$  K) prior to the experiments. The calibration data is summarized in Appendix 3.

## 4 Test matrix and data structure of Cold-Channel-Experiments

All experimental data of the Cold-Channel tests listed in Table 3 to Table 8 are published as zipped Excel-files via the PRESLHY repository on KITOpen <sup>1</sup>.

The test matrix was generated by varying the maximum hydrogen concentration in the channel for two hydrogen temperature levels in the cooling tube (approx. 80 K and 300 K) and three blockage ratios inside the channel (0%, 30% and 60%). The experiments are listed in six tables for experiments with the same H<sub>2</sub>-temperature and the same channel blockage ratio. In the tables, the experiments are listed according to ascending initial H<sub>2</sub>-pressure in the cooling tube ( $p_{ini}$ ), increasing injection duration ( $t_{inject}$ ) and average hydrogen content at the channel ceiling. Additionally, information on the averaged H<sub>2</sub>-concentration close to the bottom of the channel and the maximum and minimum concentrations measured are given. All hydrogen concentrations were determined in a distribution experiment prior to the separate ignition experiment, which was usually conducted immediately after the distribution experiment using the same parameter settings. Additionally the pressure difference  $\Delta p$  to the initial pressure inside the cooling tube after the H<sub>2</sub>-injection into the channel is listed, as well as the time delay  $\Delta t$  that was used before samples of the mixture in the channel were taken or the mixture was ignited ( $\Delta t$  was always the same in a set of distribution and combustion experiments). In further three columns the names of the different data files of an experiment are listed. Slow LabView data acquisition was used in distribution as well as in combustion experiments, whereas the fast data acquisition for the pressure sensors, open thermocouples and ionization probes was only utilized in the combustion experiments. In the last two columns the names of the High-speed- and Thermocamera-video files are listed, that are published together with the experimental data.

The experimental data in the archive is divided into six zip-files according to the six main cases (three blockage ratios and two temperatures) used in the Cold-Channel experiments, (Figure 15).

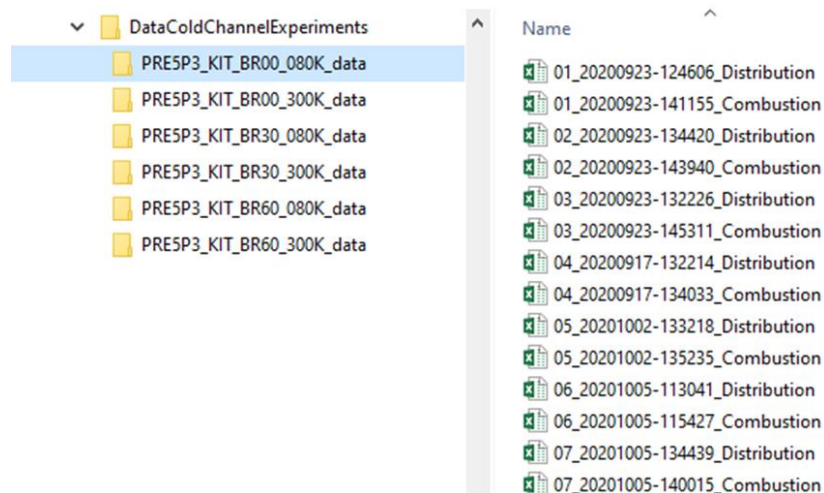


Figure 15: Folder structure for the experimental data in the zip-archive.

<sup>1</sup> <https://www.bibliothek.kit.edu/cms/english/kitopen.php>

Table 3: Test matrix of the Cold-Channel experiments at 80K with a blockage ratio of 0% (unobstructed channel)

Exp. No.	Injection – cH2/Ignition				cH2 [Vol%]				Data Files			Video files	
	p <sub>ini</sub> [bar]	t <sub>inject</sub> [ms]	Δp [bar]	t <sub>Delay</sub> [ms]	Top (Avg.)	Botm (Avg.)	Max	Min	LabView (Distribution)	LabView (Combustion)	Fast Acquisit. (P, OT, IP)	High-Speed Camera	Thermocamera
1	10.8	500	1.9	2000	8.7	6.4	14.3	2.4	20200923-124606	20200923-141155	20200923-17	cold10_br0_bosfirecode.avi	
2	10.8	600	2.3	2000	8.1	4.9	14.2	1.7	20200923-134420	20200923-143940	20200923-18		
3	10.8	750	2.9	2000	14.9	6.7	19.6	4.4	20200923-132226	20200923-145311	20200923-19	cold15_br0_imgadjusted.avi	
4	10.8	750	2.7	2000	17.3	5.0	18.8	2.1	20200917-132214	20200917-134033	20200917-09		IR_17-09-2020_0002.csq
5	10.8	2200	6.7	2000	31.7	8.0	35.6	5.1	20201002-133218	20201002-135235	20201002-23	cold30_br0_bosfirecode.avi	IR_02-10-2020_0001/0003.csq
6	11.1	5000	10.4	2000	44.7	17.7	48.6	6.1	20201005-113041	20201005-115427	20201005-24	cold43_br0_bosblue.avi	
7	22.1	7000	21.5	2000	57.1	29.4	58.8	20.8	20201005-134439	20201005-140015	20201005-25	cold55_br0_bosfirecode.avi	

Table 4: Test matrix of the Cold-Channel experiments at 300K with a blockage ratio of 0% (unobstructed channel)

Exp. No.	Injection – cH2/Ignition				cH2 [Vol%]				Data Files			Video files	
	p <sub>ini</sub> [bar]	t <sub>inject</sub> [ms]	Δp [bar]	t <sub>Delay</sub> [ms]	Top (Avg.)	Botm (Avg.)	Max	Min	LabView (Distribution)	LabView (Combustion)	Fast Acquisit. (P, OT, IP)	High-Speed Camera	Thermocamera
1	13.8	400	3.8	2000	9.8	2.4	10.3	1.3	20200922-105752	20200922-112514	20200922-10		
2	13.4	500	4.5	2000	10.5	1.8	12.2	0.5	20200918-115456	20200922-115530	20200922-11		
3	13.6	800	6.6	2000	13.9	3.3	15.9	1.4	20200918-130623	20200922-125810	20200922-13	warm10_br0_bosblue.avi	
4	13.6	900	7.2	2000	15.8	3.8	17.1	1.8	20200922-120546	20200922-124602	20200922-12	warm15_br0_bosblue.avi	
5	13.8 13.6 13.7	3500	13.4 13.3 13.3	2000	31.9	5.2	32.8	2.6	20200922-133831	20200922-135552 and -142532 and -150117	20200922-14 and -15 and -16	warm30_br0_bosfirecode_01/ 02.avi	
6	28.1 28.0	5000	28.8 28.7	2000	45.3	8.4	46.5	2.8	20200924-135226	20200924-152403 and -161801	20200924-20 and -21	warm44_br0_bosblue/firecode _01/02.avi	IR_24-09-2020_0002/0003.csq
7	61.5 61.5	12000	62.4 62.4	2000	56.6	16.9	57.9	14.9	20201001-134152	20201001-142721 20201001-145110	Record failed 20201001-22	warm55_br0_bosblue.avi	IR_01-10-2020_0002/0003.csq

Table 5: Test matrix of the Cold-Channel experiments at 80K with a blockage ratio of 30%

Exp. No.	Injection – cH2/Ignition				cH2 [Vol%]				Data Files			Video files	
	$p_{ini}$ [bar]	$t_{inject}$ [ms]	$\Delta p$ [bar]	$t_{Delay}$ [ms]	Top (Avg.)	Botm (Avg.)	Max	Min	LabView (Distribution)	LabView (Combustion)	Fast Acquisit. (P, OT, IP)	High-Speed Camera	Thermocamera
1	11.4	300	1.0	2000	8.0	2.0	12.6	0.6	20201019-120450	20201019-122743	20201019-36		IR_19-10-2020_0002.csq
2	10.9	350	1.4	2000	8.8	6.6	15.3	1.3	20201013-123818	20201013-135627	20201013-34		
3	11.4	350	1.2	2000	12.8	2.5	20.6	1.0	20201019-131315	20201019-133335	20201019-37	cold10_br30_bosfirecode.avi	IR_19-10-2020_0003.csq
4	11.3	400	1.4	2000	16.1	6.4	20.0	3.5	20201019-124351	20201019-134952	20201019-38		IR_19-10-2020_0004.csq
5	11.4	400	1.5 1.6	2000	12.9 15.4	2.6 2.6	15.3 21.0	2.2 0.5	20201022-122210 20201022-124855	20201022-130846	20201022-48		
6	11.4	450	1.5	2000	14.7	1.3	22.4	1.1	20201019-144727	20201019-150251	20201019-39		IR_19-10-2020_0005.csq
7	11.4	500	2.2	2000	18.7	3.8	20.7	1.8	20201022-133321	20201022-135441	20201022-49	cold15_br30_bosblue.avi	
8	11.4	500	2.7	2000	21.2	3.0	23.3	1.3	20201022-143103	20201022-141622	20201022-50		
9	11.4	600	2.4	2000	23.4	2.8	28.3	1.2	20201022-145458	20201022-151236	20201022-51		
10	11.4	700	2.1	2000	22.1	4.2	23.6	3.0	20201027-121837	20201027-123504	20201027-56		IR_27-10-2020_0002.csq
11	11.4	800	2.9	2000	25.7	8.3	28.2	2.6	20201027-130914	Record failed 20201027-133903	20201027-57 and -58		IR_27-10-2020_0003/0004.csq
12	11.4	900	2.9	2000	23.6	5.6	30.9	1.7	20201027-143436	20201027-145553	20201027-59	cold25_br30_bosfirecode.avi	IR_27-10-2020_0005.csq
13	11.0	1000	3.9	2000	22.1	8.8	25.3	5.7	20201013-144135	20201013-150514	20201013-35		

Table 6: Test matrix of the Cold-Channel experiments at 300K with a blockage ratio of 30%

Exp. No.	Injection – cH2/Ignition				cH2 [Vol%]				Data Files			Video files	
	P <sub>ini</sub> [bar]	t <sub>inject</sub> [ms]	Δp [bar]	t <sub>Delay</sub> [ms]	Top (Avg.)	Botm (Avg.)	Max	Min	LabView (Distribution)	LabView (Combustion)	Fast Acquisit. (P, OT, IP)	High-Speed Camera	Thermocamera
1	13.4	400	4.0	2000	11.9	1.2	14.6	0.8	20201008-123728	20201008-130235	20201008-26		
2	13.8	400	4.1	2000	12.0	4.0	14.8	2.8	20201008-105944	20201008-132319	20201008-27		
3	13.9	550	5.2	2000	14.5	5.1	17.0	3.6	20201008-142519	20201008-144723	20201008-28		
4	13.8 13.9	700	6.3 6.3	2000	17.6	3.1	21.2	0.9	20201008-140554	20201008-150335 and -152121	Record failed 20201008-30		
5	13.9	2500	12.9	2000	30.8	4.5	34.1	3.1	20201009-104121	20201009-105835	20201009-31	warm30_br30_bosblue.avi	
6	16.8	100	1.2	2000	6.6	0.5	8.7	0.4	20201020-100018	20201020-110942	20201020-40		
7	16.8	200	2.2	2000	9.2	1.2	10.8	0.4	20201020-112551	20201020-114612	20201020-41	warm10_br30_bosfirecode.avi	
8	16.8	300	3.5	2000	13.4	0.9	14.7	0.6	20201020-125108	20201020-132011	20201020-42		
9	16.8	400	4.8	2000	17.2	0.9	17.9	0.6	20201020-134113	20201020-140405	20201020-43	warm15_br30_bosblue.avi	
10	16.8	500	5.6	2000	19.2	2.1	21.8	0.7	20201021-125514	20201021-131722	20201021-45		IR_21-10-2020_0002.csq
11	16.8	500	5.9	2000	20.6	1.6	21.9	0.7	20201020-142322	20201020-145606	20201020-44		
12	16.8	600	6.4	2000	22.6	2.8	22.9	0.8	20201021-133528	20201021-135437	20201021-46		IR_21-10-2020_0003.csq
13	16.9	700	7.3	2000	23.7	2.2	27.0	0.5	20201021-143315	20201021-145300	20201021-47		IR_21-10-2020_0004.csq
14	16.8 16.8	800	8.0 8.0	2000	24.9	3.0	25.8	1.7	20201023-104929	20201023-110623 and -114358	20201023-52 and -53		IR_23-10-2020_0002/0003.csq
15	16.8	900	8.8	2000	27.1	3.2	27.4	1.1	20201023-121549	20201023-123646	20201023-54	warm25_br30_imgshadow.avi	IR_23-10-2020_0004.csq
16	16.8	1000	9.6	2000	29.8	2.6	31.5	1.7	20201023-130159	20201023-132208	20201023-55		IR_23-10-2020_0005.csq
17	27.8	4000	27.6	2000	45.6	13.9	47.9	1.0	20201009-125532	20201009-131456	20201009-32	warm44_br30_imgshadow.avi	

Table 7: Test matrix of the Cold-Channel experiments at 80K with a blockage ratio of 60%

Exp. No.	Injection – cH2/Ignition				cH2 [Vol%]				Data Files			Video files	
	P <sub>ini</sub> [bar]	t <sub>inject</sub> [ms]	Δp [bar]	t <sub>Delay</sub> [ms]	Top (Avg.)	Botm (Avg.)	Max	Min	LabView (Distribution)	LabView (Combustion)	Fast Acquisit. (P, OT, IP)	High-Speed Camera	Thermocamera
1	11.4	300	1.1	2000	7.1	2.8	11.8	0.6	20201113-121701	20201113-125316	20201113-73		
2	11.4	350	1.3	2000	9.5	2.4	16.1	0.5	20201113-130459	20201113-132748	20201113-74		
3	11.4	400	1.4	2000	13.8	3.3	21.2	1.7	20201113-135005	20201113-141227	20201113-75		
4	11.4	450	1.4	2000	10.2 12.5	2.7 3.6	18.1 16.1	0.6 1.7	20201116-132117 20201116-134313	20201116-141828	20201116-78	cold10_br60_bosblue.avi	IR_16-11-2020_0001.csq
5	11.5	500	11.8	2000	16.2	3.2	23.5	2.8	20201113-142356	20201113-144650 and -150742	20201113-76 and -77	cold15_br60_bosblue_01/02.avi	
6	11.5	600	2.0	2000	17.0	1.6	22.7	0.5	20201116-143451	20201116-145301	20201116-79		IR_16-11-2020_0003.csq
7	11.4	700	2.3	2000	19.9	3.9	24.5	3.3	20201119-125135	20201119-133305	20201119-82		IR_19-11-2020_0002.csq
8	11.5	700	2.3	2000	20.9	6.9	25.3	5.6	20201116-153012	20201116-155101	20201116-80		IR_16-11-2020_0004.csq
9	11.4	700	2.0	2000	26.9	2.7	32.3	1.2	20201119-120219	20201119-122329	20201119-81		IR_19-11-2020_0001.csq
10	11.4	800	?	2000	24.2	3.6	30.5	3.3	20201119-135854	20201119-143308	20201119-83		IR_19-11-2020_0003.csq
11	11.4	900	?	2000	26.5	6.2	33.5	3.5	20201119-155441	20201120-124555	20201120-84		IR_20-11-2020_0001.csq
12	11.5 11.4	1000	3.1 3.3	2000	23.9 26.0	5.7 6.4	30.3 35.4	3.2 2.6	20201126-121143 20201124-122326	20201124-153353	20201124-85	cold25_br60_imgshadow.avi	
13	11.5	1250	4.4	2000	27.9	9.5	34.1	7.2	20201126-123722	20201126-132425	20201126-86		
14 15	11.5	1500 1600	5.3 5.4	2000	30.5 30.7	15.2 12.6	36.2 36.0	10.5 8.1	20201126-144720 20201126-151002	20201126-152620	20201126-87	cold30_br60_imgshadow.avi	

Deviations larger than 1 bar in between distribution and combustion experiment

Table 8: Test matrix of the Cold-Channel experiments at 300K with a blockage ratio of 60%

Exp. No.	Injection – cH2/Ignition				cH2 [Vol%]				Data Files			Video files	
	p <sub>ini</sub> [bar]	t <sub>inject</sub> [ms]	Δp [bar]	t <sub>Delay</sub> [ms]	Top (Avg.)	Botm (Avg.)	Max	Min	LabView (Distribution)	LabView (Combustion)	Fast Acquisit. (P, OT, IP)	High-Speed Camera	Thermocamera
1	16.8	200	2.3	2000	6.3	1.0	11.8	0.6	20201030-114405	20201030-120645	20201030-60		
2	16.8	300	2.9	2000	10.6	2.3	14.2	0.6	20201030-122557	20201030-124352	20201030-61	warm10_br60_bosblue.avi	IR_30-10-2020_0002.csq
3	16.8	300	3.1	2000	11.5	1.1	13.4	0.7	20201109-104426	20201109-110348	20201109-62		
4	16.8	400	4.3	2000	13.7	1.2	18.7	0.5	20201109-112008	20201109-114245	20201109-63		
5	16.8	500	5.3	2000	16.3	1.5	22.1	0.6	20201109-115406	20201109-123903	20201109-65	warm15_br60_bosfirecode.avi	
6	16.8	600	6.6	2000	19.9	2.4	22.6	0.8	20201109-130232	20201109-132954	20201109-66		
7	16.8	700	7.1	2000	20.4 21.1	2.8 3.6	22.9 24.4	1.3 1.8	20201109-151033 20201109-135104	20201109-144007	20201109-67		
8	16.8	800	7.8	2000	22.7	3.3	28.1	1.1	20201111-124953	20201111-131416	20201111-68		IR_11-11-2020_0002.csq
9	16.8	900	8.3	2000	25.0	3.3	31.5	1.3	20201111-134950	20201111-140912	20201111-69		IR_11-11-2020_0003.csq
10	16.8	1000	9.1	2000	26.1	3.9	33.5	2.1	20201111-144259	20201111-150318	20201111-70	warm25_br60_imgshadow.avi	IR_11-11-2020_0004.csq
11	16.8	1500	12.0	2000	33.0	5.1	41.1	4.7	20201111-154036	20201111-160406	20201111-71	warm30_br60_imgshadow.avi	IR_11-11-2020_0005.csq

The naming convention of the corresponding zip-files largely follows the one provided in the Data Management Plan and reads as follows:

**PRE5P3\_KIT\_BR%%\_tttK\_extn.zip**

With %% indicating the blockage ratio ("00","30" or "80" %), **ttt** the nominal start temperature ("080" for LN2 cooling or "300" for ambient) and **extn** the type of data contained ("DATA" for Excel sheets containing all numerical and some predefined graphs, "HS" and "TH" for videos with either the High-Speed- or the THERmocamera). In the zip-files the data files are assorted according to the case-number given in the first column of the respective test matrix (Table 3 to Table 8) and for every case at least two experiments were conducted: one distribution and one combustion experiment (in case of repetitions an additional letter is added to the case number). The filenames all have the following structure

**CC\_2020MMDD-hhmmss-Distribution/Combustion**

In which **CC** is the case number (first column of the respective test matrix in Table 3 to Table 8), and **MM**, **DD**, **hh**, **mm** and **ss** are the month, day, hour, minute and second of the time the experiment was started. Additionally, at the end of the name it is indicated whether it is the distribution or the combustion experiment for the respective case.

**4.1 Structure of the Datasets**

The result data is stored in Excel files and contains the measured values of all sensors used in the facility. The Excel-files usually contain three sheets, with the third sheet being different in combustion and distribution experiments.

The first sheet in all Excel-files has the name "2020MMDD-hhmmss\_PTube" and contains the signal of the pressure sensor installed to the cooling tube (see Figure 16).

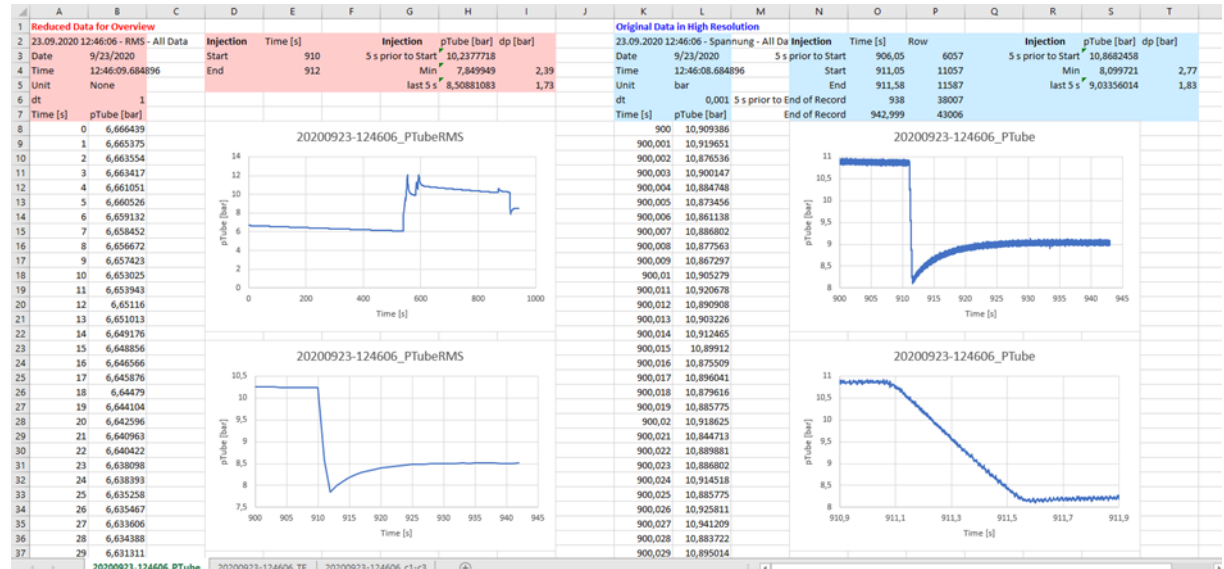


Figure 16: Example for the first sheet in the Excel file "01\_20200923-124606\_Distribution" form the folder "PRE5P3\_KIT\_BR00\_080K\_data".

On the left side a pressure record over the complete experiment duration (including tube filling) is plotted in reduced resolution (1 Hz). This graph is used to identify the time span

in which the actual experiment takes place, which is characterized by a sudden pressure decrease due to the injection of the hydrogen from the tube into the channel. On the right side the “interesting part” of the same signal is plotted in its original high resolution (1 kHz) to allow a detailed analysis of the depressurization of the cooling tube. As “interesting part” a time span from approx. 15 s prior to the pressure decrease until the end of the record was chosen.

The second sheet in all Excel-files has the name “2020MMDD-hhmmss\_TE” and contains the records of all thermocouples installed to the facility (Figure 17) for the “interesting part” of the experiment.



Figure 17: Example for the second sheet in the Excel file “01\_20200923-124606\_Distribution” form the folder “PRE5P3\_KIT\_BR00\_080K\_data”.

The records are also plotted in groups for thermocouples installed to the cooling tube (columns B, C and D, top left graph), the Cryovessel (only used in few initial experiments, columns E, F and G, second left graph) and the injection lines (columns H and I, third left graph) as well as the temperature measurements inside the channel (columns J to U, naming convention according to sketch in Figure 9, right graphs). The last column V contains data of a virtual thermocouple that was added to provide a trigger signal (when injection valve was opened) in the temperature records.

All Excel-files for distribution experiments have a third sheet with the name “2020MMDD-hhmmss\_c1-c3” that contains the results of the H<sub>2</sub>-concentration measurements performed only in these tests (Figure 18). In the two graphs the concentration measurements for the three measurements position (columns B to D, naming according to sketch in Figure 9) are listed. Usually the measurements were conducted starting with the sample that was taken close to the channel ceiling (first peak in the curve for position 1, 2 or 3), and was then continued in downward direction (following four peaks). Above the graphs the maximum values measured in the different positions are summarized and in the black box mean and extremal concentration values are calculated. The entries in the grey box were merely used during evaluation to find the rows in the data for a given point in time.

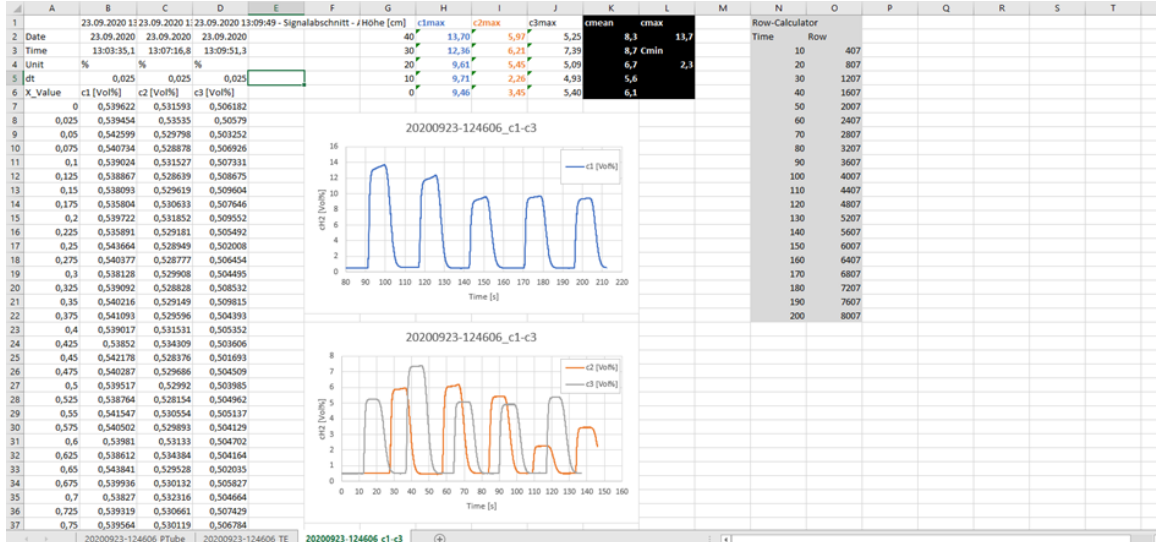


Figure 18: Example for the third sheet in the Excel file “01\_20200923-124606\_Distribution” form the folder “PRE5P3\_KIT\_BR00\_080K\_data”.

All Excel-files for combustion experiments have a third sheet with the name “2020MMDD-XX” (Figure 19, XX is the consecutive number of the experiment, compare test matrix tables) that contains the results of the fast data acquisition system, which was only used in the combustion tests. Due to the high resolution of the original records (100 kHz) the data was decimated by a factor of 10 (first-value-method) for experiments with slow flames to keep the file size acceptable, since in this case a longer time span is needed. In case of fast flames, the original resolution is used for a shorter time span.

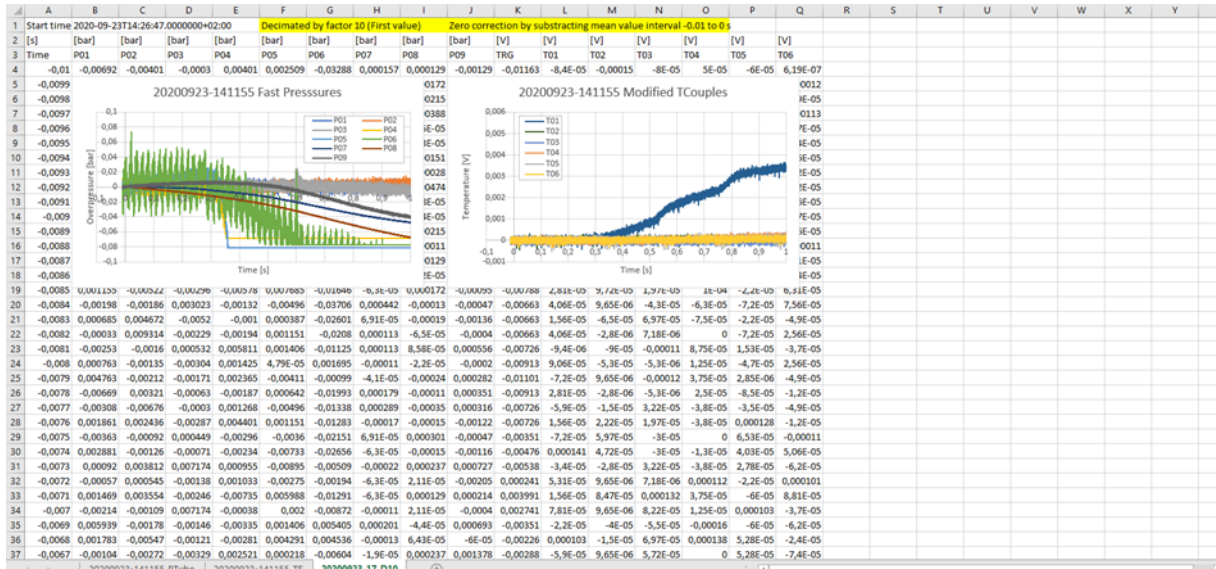


Figure 19: Example for the third sheet in the Excel file “01\_20200923-141155\_Combustion” form the folder “PRE5P3\_KIT\_BR00\_080K\_data”.

The left graph of this third sheet displays the records of the fast pressure sensors distributed along the channel ceiling and the floor below the channel (columns B to J, naming according to sketch in Figure 11). In the right graph(s) the records of the modified

thermocouples (columns K to Q) and the ionization probes (added later, columns R to W), both used for flame detection, are plotted.

## 5 Summary, Conclusions and Outlook

In the frame of the PRESLHY project more than 100 combustion experiments with cryogenic hydrogen-air-mixtures were made in a semi-confined obstructed channel. In the experiments a large H<sub>2</sub>-concentration range from 10 vol% up to 60 vol% as well as different blockage ratios (BR = 0, 30 and 60%) were investigated. Besides the main experimental series at cryogenic temperatures with pre-cooled hydrogen from the cooling tube (approx. 80 K, resulting in approx. 100 K in the channel) most of the experiments were also performed at ambient temperature for comparison.

The experimental series carried out gives a first insight into the combustion process of cryogenic inhomogeneous hydrogen-air layers in the semi-confined geometry. The measured values provide a database for the further development and validation of complex simulation tools dedicated to hydrogen safety.

Due the enormous experimental program executed by Pro-Science/KIT and the resulting lack of time the data was only processed, but not evaluated in detail up to the end of the PRESLHY project and thus no preliminary results can be presented here.

## Appendix 1 - Calibration of the sampling cylinders

Date 11.09.20

Each sampling cylinder was evacuated 2 times and connected to its corresponding cannula with a test gas balloon, as shown in Figure 10. Between the tests, the sampling line was exposed to ambient air to avoid measurement errors. With cylinder 1, reference samples were taken without cannula to capture the effect of the cannula volume. During the first series of measurements, different opening times of the inlet valve were tested (1 ms to 3000 ms) with 2000 ms being recognized as optimum and so this time was kept for the rest of the experiments.

		%Match		%Match		
		9,1	91	9,675	96,75	Test different opening hours
10:04:38	Gas mouse 1	9,652	96,52	9,705	97,05	1ms-3000ms
		9,555	95,55	9,655	96,55	
10:09:19	Gas mouse 2	9,65	96,5	9,55	95,5	
10:12:27	Gas mouse 3	9,62	96,2	9,47	94,7	
10:15:39	Gas mouse 4	9,53	95,3	9,51	95,1	
10:20:24	Gas mouse 5	defective		defective		defective
10:25:57	Gas mouse 6	9,47	94,7	9,42	94,2	
10:28:39	Gas mouse 7	9,42	94,2	9,4	94	
10:31:28	Gas mouse 8	9,34	93,4	9,35	93,5	
10:36:08	Gas mouse 9	9,35	93,5	9,35	93,5	
10:39:06	Gas mouse 10	9,358	93,58	9,35	93,5	
10:40:52	Gas mouse 11	9,24	92,4	9,31	93,1	
10:43:25	Gas mouse 12	9,33	93,3	9,33	93,3	
10:52:39	Gas mouse 1	9,15	91,5	9,154	91,54	Remark: Mouse without cable mounted on mouse with intermediate piece possibly leaking
10:58:43	Gas mouse 1	<b>9,87</b>	<b>98,7</b>			Remark: Mouse without cable mounted on mouse without adapter

## Appendix 2 - Calibration data of the pressure sensors

Two types of PCB pressure sensors with external amplifiers were used in the experiments. The sensors were once connected to an amplifier and used as a pair during the complete experimental series. For most experiments type 112A05 with amplifiers 422E52 (measuring range up to 35 bar) were used. For higher pressures eight sensors of type 116B with amplifiers 422E53 (measuring range up to 345 bar) were available. These sensors were tested and used only in very few experiments since the sensors of type 112A05 proved to be sufficient for most experiments. The calibration data provided by the manufacturer is given below for the sensor/amplifier pairs used.

### Model 112A05 with amplifiers 422E52

Sensor	Typ	7 bar Sens [pC/kPa]	35 bar LP-Sens [pC]	Verstärker	Typ	Gain [mV/pC]	Sens [mV/kPa]	7 bar Sens [mV/ba]	35 bar Sens [mV/ba]	7 bar Sens [bar/m]	35 bar Sens [bar/m]
37612	112A05	0,1601	0,1659	51813	422E52	9,892	1,5837092	158,3709	164,1083	6,3143	6,0935
6806	116B	0,8939		51804	422E53	1,005	0,8983695	89,8370		11,1313	
37617	112A05	0,1505	0,1528	51810	422E52	10,003	1,5054515	150,5452	152,8458	6,6425	6,5425
6807	116B	0,9063		51881	422E53	1,004	0,9099252	90,9925		10,9899	
37614	112A05	0,1482	0,1519	51812	422E52	9,940	1,473108	147,3108	150,9886	6,7884	6,6230
6805	116B	0,8908		51803	422E53	1,002	0,8925816	89,2582		11,2035	
37615	112A05	0,1600	0,1631	51808	422E52	9,962	1,59392	159,3920	162,4802	6,2738	6,1546
6804	116B	0,8969		51882	422E53	1,003	0,8995907	89,9591		11,1162	
37600	112A05	0,1496	0,1542	51814	422E52	9,949	1,4883704	148,8370	153,4136	6,7188	6,5183
6809	116B	0,8789		51883	422E53	1,006	0,8841734	88,4173		11,3100	
37613	112A05	0,1607	0,1637	51811	422E52	9,930	1,595751	159,5751	162,5541	6,2666	6,1518
6811	116B	0,8751		51801	422E53	1,002	0,8768502	87,6850		11,4045	
37601	112A05	0,1452	0,1504	51809	422E52	10,013	1,4538876	145,3888	150,5955	6,8781	6,6403

Modell	345 bar	34,5 bar	6,89 bar	Modell	422E52
112A05	< 5000 PSI	< 500 PSI	< 100 PSI	Ser.-Nr.	Gain [mV/pC]
Ser.-Nr.	HP-Sens [pC]	LP-Sens [pC]	VeryLP-Sens [pC/kPa]	Ser.-Nr.	Gain [mV/pC]
37600	178,7	154,2	0,1496	51808	9,962
37601	172,3	150,4	0,1452	51809	10,013
37611	158,3	166,2	0,1626	51810	10,003
37612	167,9	165,9	0,1601	51811	9,930
37613	169,5	163,7	0,1607	51812	9,940
37614	159,3	151,9	0,1482	51813	9,892
37615	169,2	163,1	0,1600	51814	9,949
37617	160,0	152,8	0,1505	51892	10,011

### Model 116B with amplifiers 422E53

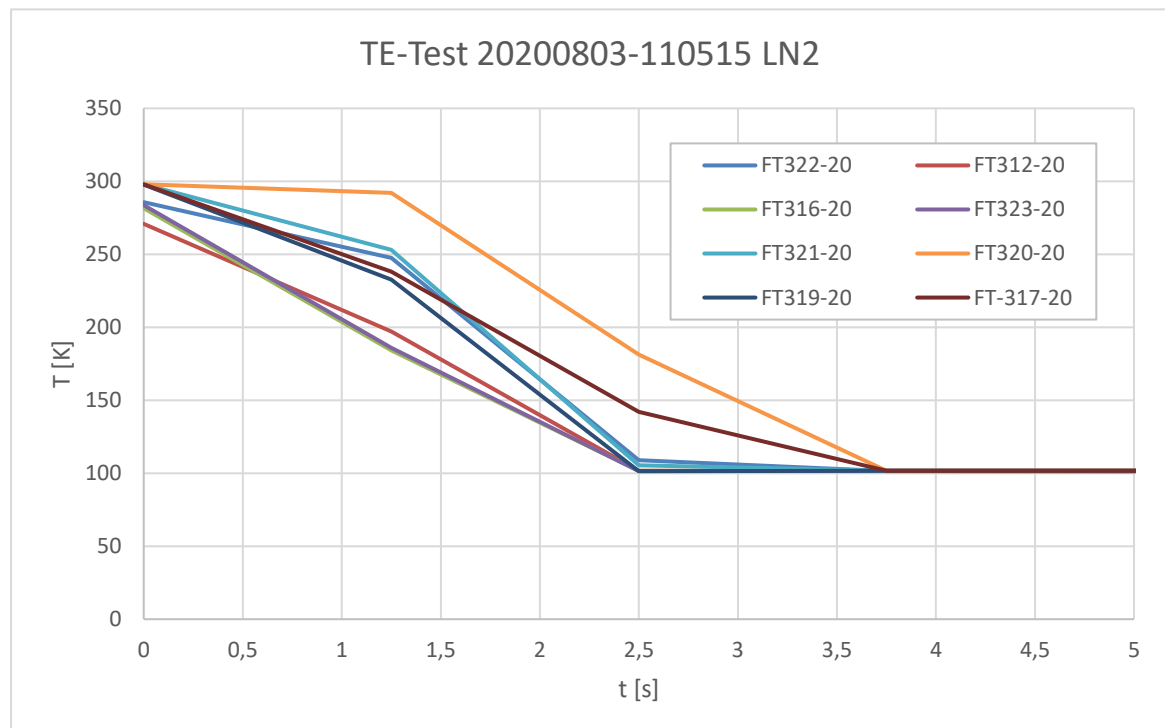
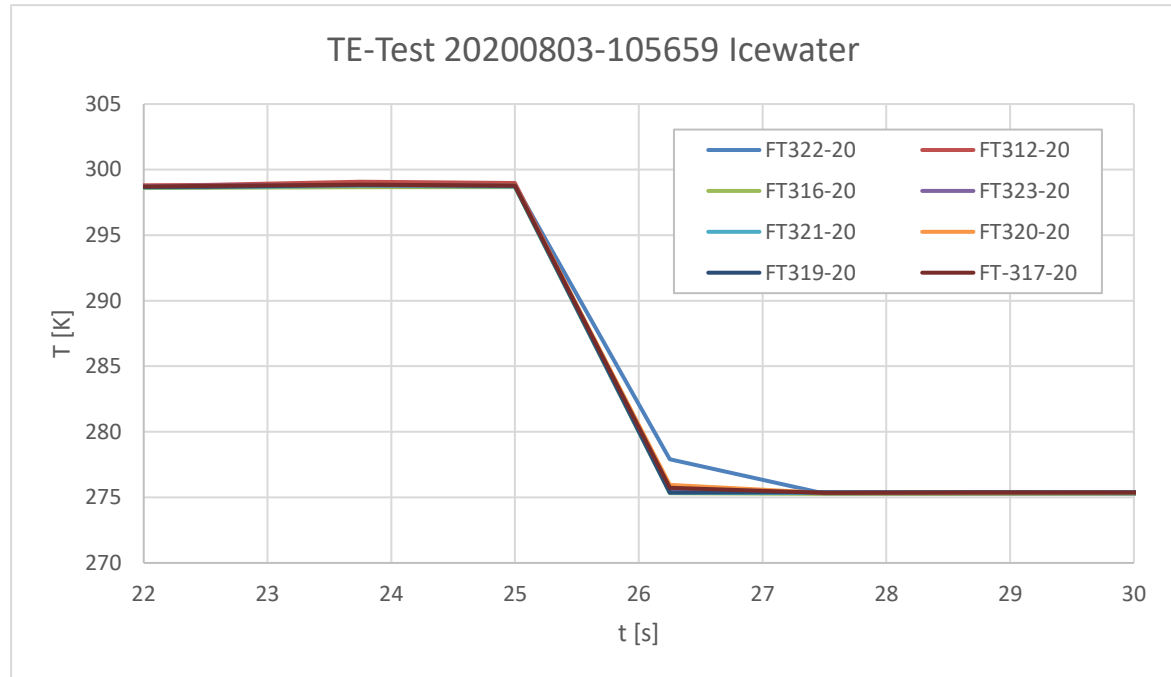
Modell	6,89 bar	Modell	422E53	
116B	< 100 PSI	Acoustic	Ser.-Nr.	
Ser.-Nr.	Sens [pC/kPa]	Sens [pC/kPa]	Gain [mV/pC]	
6804	0,8969	1,04	51801	1,002
6805	0,8908	1,04	51802	1,000
6806	0,8939	1,02	51803	1,002
6807	0,9063	1,03	51804	1,005
6808	0,9105	1,04	51880	1,005
6809	0,8789	1,00	51881	1,004
6810	0,9235	1,04	51882	1,003
6811	0,8751	1,03	51883	1,006

### Appendix 3 - Calibration of the Thermocouples

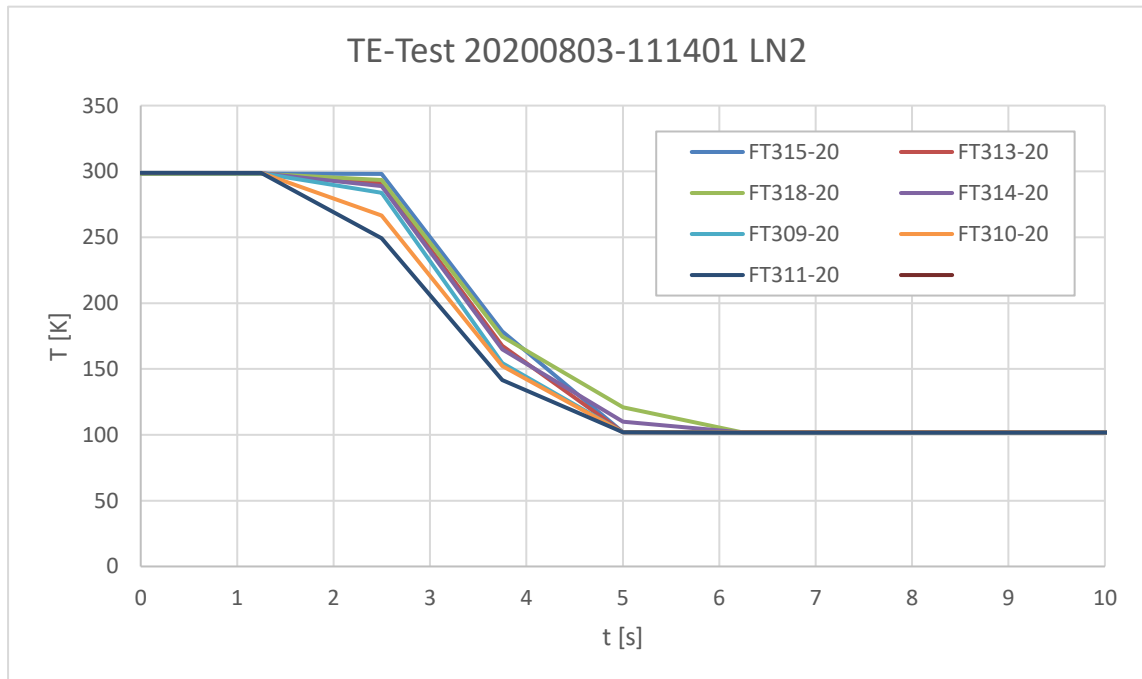
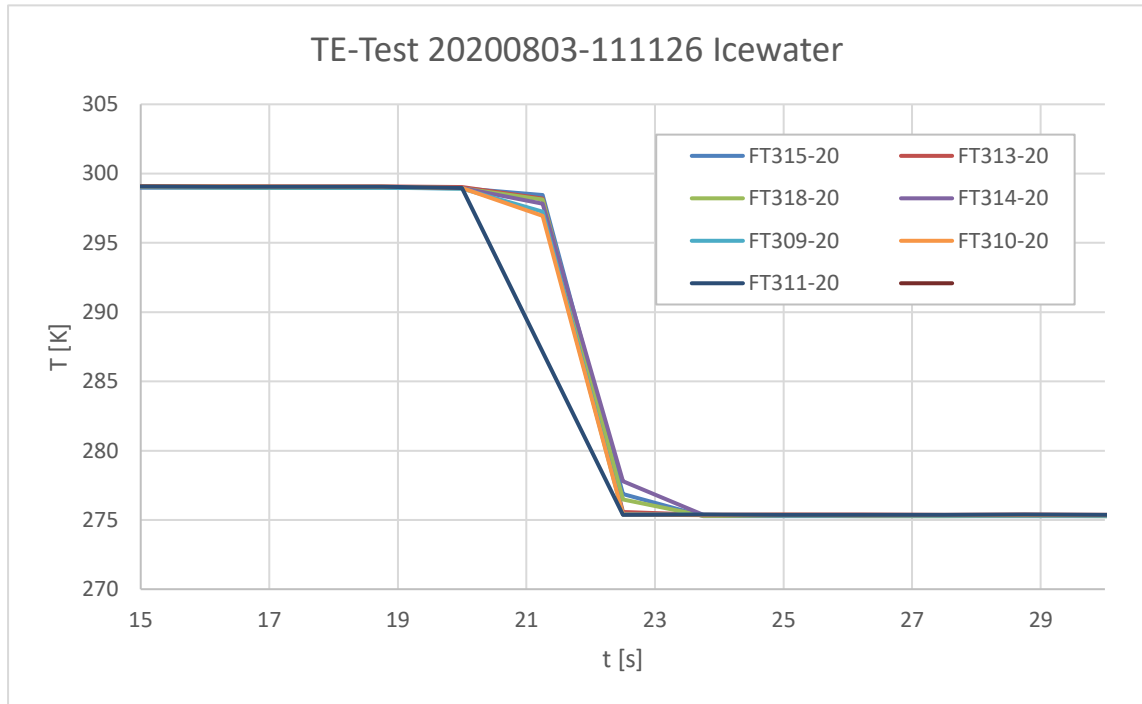
Date 03.08.20

Thermocouples of the same batch of raw material usually show the same temperature deviation. Nevertheless, all thermocouples used in the experiments were calibrated by measurements in ice water (0°C/273.15K) and in LN2 (77 K). The measurements were conducted in three groups and deviations of approx. 3 K or 23K were found in all groups for the temperature ice water and LN2, respectively.

Group 1:



Group 2:



Group 3 (single thermocouple):

